FULL PAPER

CrossMark

The afternoon counter-electrojet current system along the 75°E meridian during the IEEY

S. K. Bhardwaj and P. B. V. Subba Rao[*]

Abstract

In the present study, the technique of principal component analysis (PCA) is applied to analyze the hourly mean values of geomagnetic field components D, H, and Z along an Indo-Russian chain of stations during the International Equatorial Electrojet Year (IEEY) from January 1992 to June 1993. This technique (PCA) is found to be suitable for separating the normal electrojet (NEJ) and counter-electrojet (CEJ) variations, and the first two principal components (PCs) are able to describe the characteristics of NEJ- and CEJ-related field variations. It is found that the first principal component (PC-1) for H, D, and Z varies as a function of time with latitude and depicts the well-known Sq variations, whereas PC-2(H) does not show any variations at all latitudes during NEJ days. On CEJ days, PC-2(H) shows a large negative excursion at equatorial stations (KAN to BAN). The NEJ- and CEJ-related current systems are determined by combining the hourly inequalities in D and H. PC-1 brings out a well-defined anticlockwise loop for NEJ days, with its focus near the dip latitude (~35°N), and a clockwise loop for CEJ days with a well-defined focus near the dip latitude (~20°N) around noon local time. The CEJ-related current system is marked by intense westward current flow in the equatorial belt and is shown to close its path by forming a clockwise loop extending from the dip equator to mid-latitudes. Comparison with a numerically simulated current system, caused by various tidal modes, emphasizes the significance of antisymmetric semidiurnal tidal modes in the generation of CEJ events.

Keywords: Counter-electrojet, Sq variations, Tidal winds, Principal component analysis

Introduction

There are several electrodynamical processes that occur in the mesosphere–lower thermosphere (MLT) region over the dip equator. It is well known that the Sun emits charged particles and electromagnetic radiation that ionizes the upper atmosphere (known as the ionosphere). The motion of ionospheric plasma across the Earth's geomagnetic field under the influence of solar diurnal and semidiurnal tide-driven winds sets up dynamo currents, called the Sq current system, in the E-region of the ionosphere. It was found that the Sq variation in H was abnormally large at Huancayo Geomagnetic Observatory (established in Peru in 1922 by the Carnegie Institute of Washington), which is located near the dip equator, compared to that at the tropical latitude stations like Fuquene. This has been attributed to a band of strong

eastward current over the equator, known as the equatorial electrojet (EEJ) or normal equatorial electrojet (NEJ) (Chapman 1951). This is a large horizontal current that flows in an eastward direction at ionospheric E-region height, producing large variations in the H-component of the Earth's magnetic field. This enhancement in H may be found anywhere on Earth within $\pm 3°$ latitude on either side of the dip equator, at a height of ~106 km (Forbes 1981; Reddy 1981; Stening 1985).

To explain the mechanism of the EEJ flow and its main features (such as day-to-day and seasonal variability, the counter-electrojet, electrodynamic coupling with global-scale current systems), both theoretical and physical models of the ionospheric dynamo have been developed (Chapman and Bartels 1940; Baker and Martyn 1953; Untiedt 1967; Sugiura and Poros 1969; Richmond 1973; Kane and Trivedi 1982; Stening 1985; Reddy 1989; Abbas et al. 2012; Guizelli et al. 2013; Rastogi et al. 2013;). Dynamo models have been able to explain the solar and lunar modulations of EEJ strength, including

*Correspondence: srao@iigs.iigm.res.in
Indian Institute of Geomagnetism, Kalamboli Highway, New Panvel (W), Navi Mumbai 410 218, India

seasonal changes and variations related to the solar cycle (Reddy 1989). EEJ characteristics have been simulated by assuming a line current (Forbush and Casaverde 1961), a thin-band current with uniform and parabolic modes of latitudinal dependence (Chapman 1951), a "fourth-degree" current distribution (Fambitakoye and Mayaud 1976), and a "thick" current distribution incorporating latitude and height dependence (Onwumechili 1967). All these studies have indicated that the EEJ exhibits significant diurnal, seasonal, day-to-day, and longitudinal variabilities.

During late 1970s, the analysis of Magsat data resulted in an increased interest in these EEJ studies (Langel et al. 1982; Yanagisawa and Kono 1985; Cohen and Achache 1990; Langel et al. 1993; Ravat and Hinze 1993; Jadhav et al. 2002). Following Cain and Sweeney (1973), a number of investigations have been carried out using POGO data (Onwumechili 1997, and references therein), which have shown that the longitudinal variation of EEJ strength cannot be accounted by the longitudinal changes in the Cowling conductivity. Apart from conductivity, atmospheric tidal modes play an important role in defining the zonal variability of the EEJ current system, as suggested by Jadhav et al. (2002) using Oersted satellite data. Recently, the SWARM satellite has been launched to study and identify the different magnetic signals that arise due to the Earth's core, mantle, crust, oceans, ionosphere, and magnetosphere (Friis-Christensen et al. 2008; Macmillan and Olsen 2013; Olsen et al. 2013). Magnetic measurements from the CHAMP, Oersted, and SAC-C satellites have provided unprecedented longitudinal coverage of the EEJ. The climatological model provides the mean and variance of the EEJ as a function of longitude, local time, season, solar flux, and lunar local time (Alken and Maus 2007).

Sometimes the flow of the overhead current system reverses its direction temporarily and flows westward, producing depressions in the H-field at equatorial stations in the morning/afternoon hours during magnetically quiet days. This is known as a counter-equatorial electrojet (CEJ) (Gouin 1962; Gouin and Mayaud 1967). This was first observed by Bartels and Johnston (1940) and named a "counter-electrojet" (CEJ) by Gouin and Mayaud (1967). A CEJ can be identified by plotting the latitudinal profile of H, which will show minima instead of maxima near the dip equator. It can also be identified by taking the difference between the H-component of the geomagnetic field at an equatorial station, e.g., Trivandrum (TRD), and an off-equatorial station, e.g., Alibag (ABG);if the difference falls below the night time level, a CEJ is deemed to be present (Maynard 1967). The other two techniques used for identifying a CEJ (on quiet days) are: (1) ΔH at an EEJ station will be negative as compared

to an off-EEJ station along the same longitude, and (2) latitudinal profiles of ΔH and ΔZ from a chain of stations across the dip equator will be reversed.

The occurrence of a CEJ during quiet days has been attributed to the tidal winds or additional current systems in the ionospheric dynamo region (Bhargava and Sastri 1977; Bhargava et al. 1980; Rastogi et al. 1992; Arora et al. 1993; Somayajulu et al. 1993a; Stening et al. 1996; Alex and Mukherjee 2001; Gurubaran 2002; Sridharan et al. 2002; Chandrasekhar et al. 2017). The signature of the CEJ over the Indian sector has been illustrated by Vichare and Rajaram (2011) using Oersted satellite data. The salient features of the CEJ are:

- Gouin (1962) and Gouin and Mayaud (1967) defined a CEJ as a narrow band of currents flowing westward within the latitudes of the normal eastward EEJ currents, which causes depressions in ΔH near the magnetic equator (on a quiet day). Rastogi et al. (2007) have confirmed the above observations (reversal of ionospheric electric field during a CEJ) by correlating day-to-day changes in the midday drift at Thumba (8.55°N, 76.86°E) with the difference in ΔH-variations between Trivandrum and Alibag.

- During a quiet time CEJ, it has been observed that the electric field reverses its direction (Fejer et al. 1976), and this phenomenon has been explained by the ionospheric dynamo caused by atmospheric tidal motions (Rastogi 1974; Somayajulu et al. 1993a). Tidal winds in the east–west (zonal) direction play a significant role in the midlatitudes as compared to the equatorial region (Richmond 1973; Anandarao 1976; Reddy and Devasia 1981). Wind shears originating in gravity waves can influence the electrojet by changing its structural features to a greater extent than tidal winds do (Anandarao and Raghavarao 1987). It is shown by Raghavarao and Anandarao (1980) that a simple vertical wind of sufficient magnitude is capable of reversing an EEJ, accounting for the afternoon counter-electrojet phenomenon.

- It has been shown by many authors (Sastry and Jayakar 1972; Rastogi et al. 1975; Rangarajan and Rastogi 1981; Manju and Viswanathan 2005) that the amplitude of the solar flare effect (SFE) on the H-component decreases progressively with latitude from the equator to stations located outside the EEJ. Manju et al. (2009) have studied the effect of solar flares on geomagnetic field variations (longitudinal variability) at and around the geomagnetic equator and attribute a partial CEJ to increased ionization produced by flare-related EUV flux enhancement.

- There is an alternative interpretation of the afternoon counter-electrojet, based on the semidiurnal tide

propagating in the dynamo region on certain days. Takeda and Maeda (1981) showed that the three-dimensional currents caused by semidiurnal tidal winds, in particular of (2, 2) mode, are sufficiently intense to cause a counter-electrojet at the equator and are directed westward in the afternoon hours. There are two different views on CEJ variations. Firstly, a combination of tidal modes, in particular the (1, −2), (2, 2), and (2, 4) modes, could generate the reverse current at the magnetic equator, causing the negative perturbation in the ground magnetic field variations (Stening 1977; Marriot et al. 1979; Singh and Cole 1987; Gurubaran 2002). Secondly, Anandarao (1976) and Vineeth et al. (2007; 2009) suggest that a combination of gravity wave–tidal interactions, caused by enhanced planetary wave activity, is responsible. The interaction of upward propagation of the lower atmospheric waves with tidal components is proposed to be the mechanism for the occurrence of the CEJ.

During the International Equatorial Electrojet Year (IEEY) (January 1992–June 1993), a network of magnetometers was operated in Brazil (Rigoti et al. 1999), India (Arora et al. 1993), West Africa (Amory-Mazaudier et al. 1993; Doumouya et al. 1998; Vassal et al. 1998), and elsewhere. The latitudinal structures of the EEJ and

its day-to-day, seasonal, and longitudinal variability in each of these regions have been reported by Arora et al. (1993), Rigoti et al. (1999) and Doumouya et al. (1998; 2003). Arora et al. (1993) have utilized the 1992 IEEY datasets for the Indian sector to study the latitudinal structure of the EEJ and CEJ and their return currents.

The present paper focuses on the day-to-day variability in the NEJ and CEJ strength along an Indo-Russian chain of stations (~75°E meridian) using the principal component analysis (PCA) method for the 1992 IEEY datasets. In our analysis, we have utilized datasets from 18 permanent and temporary observatories in the Indo-Russian region to get a clear picture of the NEJ and CEJ and their latitudinal extent. The geographic and geomagnetic coordinates, together with the IAGA code and dip latitude for all the permanent and temporary geomagnetic observatories operated during the IEEY, are shown in Table 1. The locations of these stations are shown in Fig. 1 along with the dip equator.
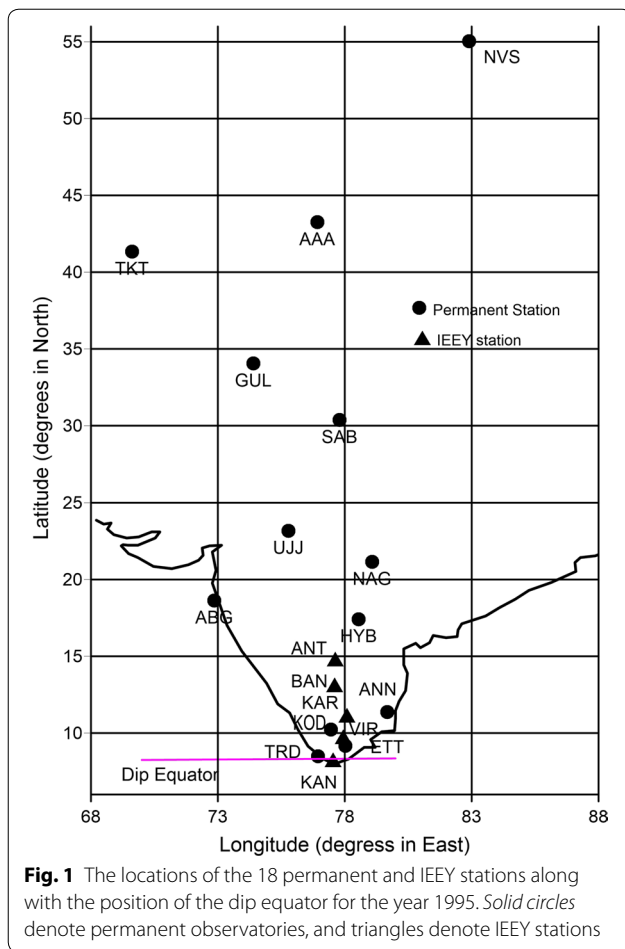
Data selection and methodology

The data used were hourly mean values of the D-, H-, and Z-components of the geomagnetic field data, on five quiet days in January and February 1992, from the 18 stations of the Indo-Russian chain. The data were corrected for non-cyclic variations and interpolated to local time (LT) for all three components. The days selected were

Table 1 List of IEEY and other stations along the Indian sector and their geographic/geomagnetic coordinates and dip latitudes

Observatory name	IAGA code	Geographic		Geomagnetic		Dip latitude (°N)
		Latitude (°N)	Longitude (°E)	Latitude (°N)	Longitude (°E)	
Novosibirsk	NVS	55.03	82.90	44.92	159.07	58.90
Alma Ata	AAA	43.25	76.92	33.69	152.21	43.50
Tashkent	TKT	41.33	69.62	32.51	145.52	41.50
Gulmarg	GUL	34.05	74.40	24.90	148.84	32.11
Sabhawala	SAB	30.37	77.80	20.93	151.50	27.35
Ujjain	UJJ	23.18	75.78	13.97	148.83	18.42
Nagpur	NAG	21.15	79.08	11.64	151.74	15.74
Alibag	ABG	18.63	72.86	9.74	145.55	12.96
Hyderabad	HYB	17.42	78.55	7.97	150.87	11.16
Anantapur[a]	ANT	14.67	77.63	5.32	149.71	7.83
Bangalore[a]	BAN	12.98	77.60	3.64	149.52	5.75
Annamalainagar	ANN	11.37	79.68	1.85	151.39	3.67
Karur[a]	KAR	11.01	78.09	1.64	149.80	3.32
Kodaikanal	KOD	10.23	77.46	0.92	149.11	2.37
Virudhunagar[a]	VIR	9.61	77.94	0.26	149.52	1.61
Ettiapuram	ETT	9.17	78.02	−0.19	149.56	1.06
Trivandrum	TRD	8.48	76.95	−0.77	148.44	0.28
Kanyakumari[a]	KAN	8.10	77.54	−1.21	148.98	−0.23

[a] IEEY stations

Fig. 1 The locations of the 18 permanent and IEEY stations along with the position of the dip equator for the year 1995. *Solid circles* denote permanent observatories, and triangles denote IEEY stations

January 21–25 and February 5, 6, 11, 15, and 16; for all of these, Ap ≤7, indicating that they were quiet days.

The method of natural orthogonal components (MNOCs) or principal component analysis (PCA) is a well-known technique applied in the field of geomagnetism to separate normal and abnormal field variations (Vertlib and Wagner 1970; Faynberg 1975; Rajaram 1980). The first principal component contains information about Sq and the electrojet, while the second component contains the counter-electrojet and disturbance field variations. Details of the MNOC are described by Reyment and Joreskog (1993). Golovkov et al. (1978) used this technique to separate the normal daily geomagnetic Sq variations from the disturbance field and found that the first component represents the actual pattern of the Sq field on a given day. PCA has been used by: (a) Bhardwaj et al. (2015) to separate normal and abnormal Sq variations; (b) Yamada (2002) to extract different oscillations from day-to-day variations at the Chichijima observatory; (c) Xu and Kamide (2004) to decompose daily magnetic variations; (d) Gurubaran (2002) to study the CEJ phenomenon and return currents on quiet days in
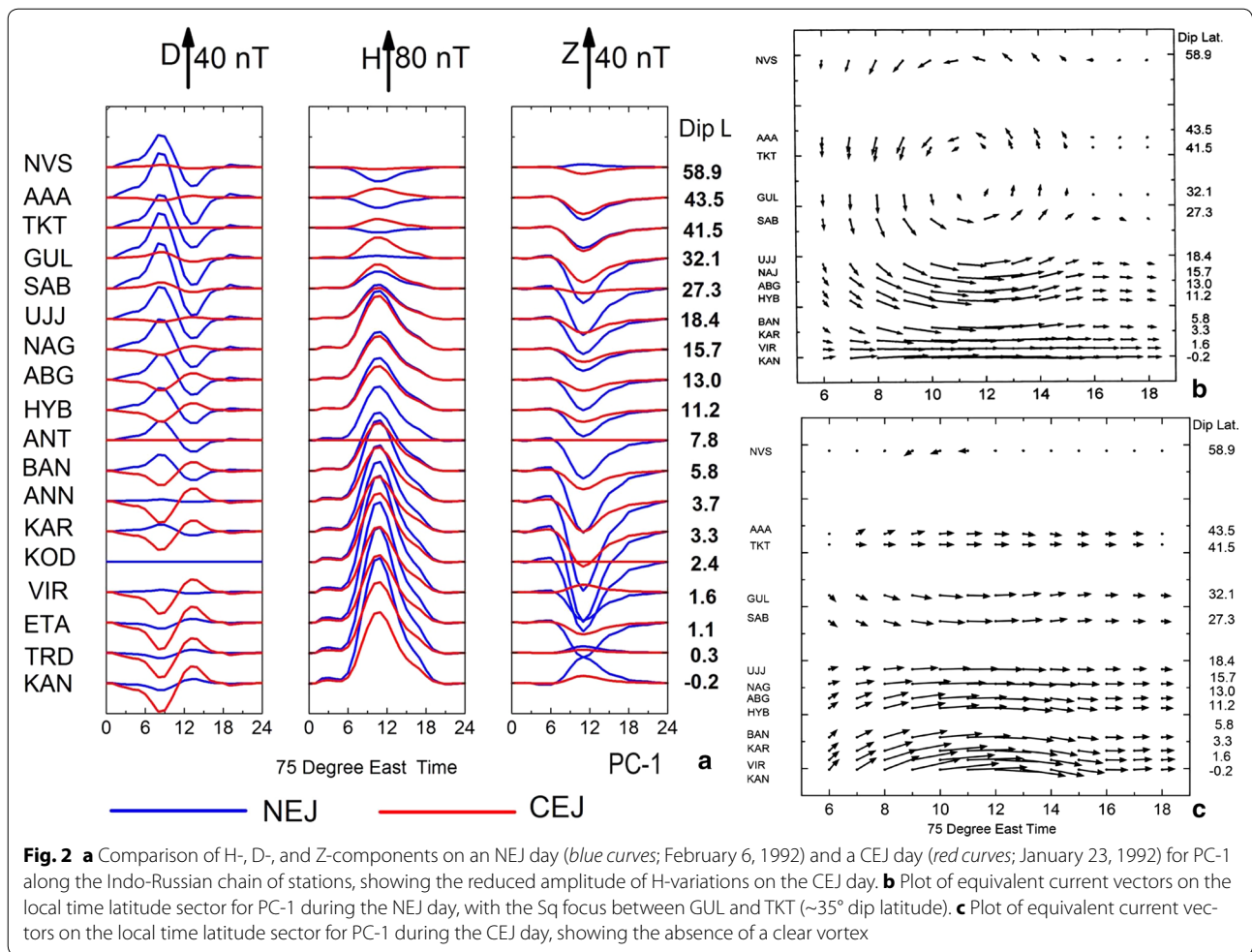
July 1995; and (e) Alex et al. (1998) to examine day-to-day variability in the equatorial electrojet strength on days of low equatorial ΔH in the Indian region. In the present study, PCA is used to analyze the hourly mean values of the D-, H-, and Z-components, in order to study the NEJ and CEJ variations. This method is useful for isolating the independent modes of variations that can account for the major parts of the variability within a given set of data.

Results

Characteristics of the NEJ and CEJ along the Indo-Russian chain of stations

Figure 2a shows diurnal variation plots of D, H, and Z corresponding to the first principal component (PC-1) for a normal electrojet day (NEJ, blue curve, February 6, 1992) and an afternoon counter-electrojet day (CEJ, red curve, January 23, 1992) for 18 stations along the 75°E meridian. They are arranged in the order of latitude and portray the expected Sq behavior for an NEJ with local time and latitude. At equatorial stations (KAN & TRD), H-variations for PC-1 are large and "inverted V"-type variations are observed with noon maxima. The amplitude of these variations decreases gradually with increasing latitude. The latitude at which the H waveform reverses its sign from "inverted V" to "V-shaped" determines the latitude of the Sq focus. As shown in Fig. 2a, the variation in the H-field reverses its sign between GUL and TKT, and stations above these latitudes are characterized by "V-shaped" variations with minima around local noon. D-variations exhibit the expected easterly maxima in the morning hours (08:00 LT) and minima in the early afternoon. However, the magnitude of the D-variations is small and reverses in direction near the dip equator, undergoing a systematic increase with increasing latitude. Figure 2b shows an equivalent current vector plot obtained by plotting the resultant of the amplitude of D- and H-variations for each hour at every observatory, and the resultant magnetic vector is rotated 90° clockwise to yield the equivalent current vector with Sq focus situated between GUL and TKT.

According to Stening and Reztsova (2007), the Z-variations largely arise from the gradient with the latitude in the eastward current flow that is detected by H-variations. As TRD is an equatorial station, the Z-variations are expected to be small. Z is nearly zero at TRD and is in opposite phases at its adjacent stations KAN and ETA, indicating that the central axis of the NEJ is close to TRD. Large Z-variations that are observed within the electrojet belt (ETA-ANN) may arise due to a subsurface electrical conductivity distribution that give rise to internal induced currents, separate from the effect of the spatial structure of the source currents. The South Indian Peninsula is known as a highly anomalous region for electrical conductivity distribution (Thakur et al. 1986; Arora and

Fig. 2 a Comparison of H-, D-, and Z-components on an NEJ day (*blue curves*; February 6, 1992) and a CEJ day (*red curves*; January 23, 1992) for PC-1 along the Indo-Russian chain of stations, showing the reduced amplitude of H-variations on the CEJ day. **b** Plot of equivalent current vectors on the local time latitude sector for PC-1 during the NEJ day, with the Sq focus between GUL and TKT (~35° dip latitude). **c** Plot of equivalent current vectors on the local time latitude sector for PC-1 during the CEJ day, showing the absence of a clear vortex

Subba Rao 2002). Both H- and Z-variations at stations located towards the south of the Sq focus increase up to BAN, due to the eastward flowing current. Above the Sq focus, H- and Z-variations decrease due to the westward flowing current on NEJ days. According to Thakkur and Alex (1977), the horizontal intensity has negative ranges for stations located north of the Sq focus and positive ranges for stations located south of the Sq focus, and this has been attributed to westward and eastward current flow. For northern hemisphere stations, the positive variation in D results from a relatively eastward magnetic field caused by a southward current in the morning. The negative variations correspond to a relatively westward magnetic field caused by a northward current in the afternoon hours, from BAN to NVS.

Both the H and D plots in Fig. 2a undergo characteristic changes on CEJ days (red curves). The amplitudes of H-variations are low and decrease with increasing latitude. However, in contrast to the NEJ days (blue curves), this decreasing trend in the H-amplitude continues right up to the la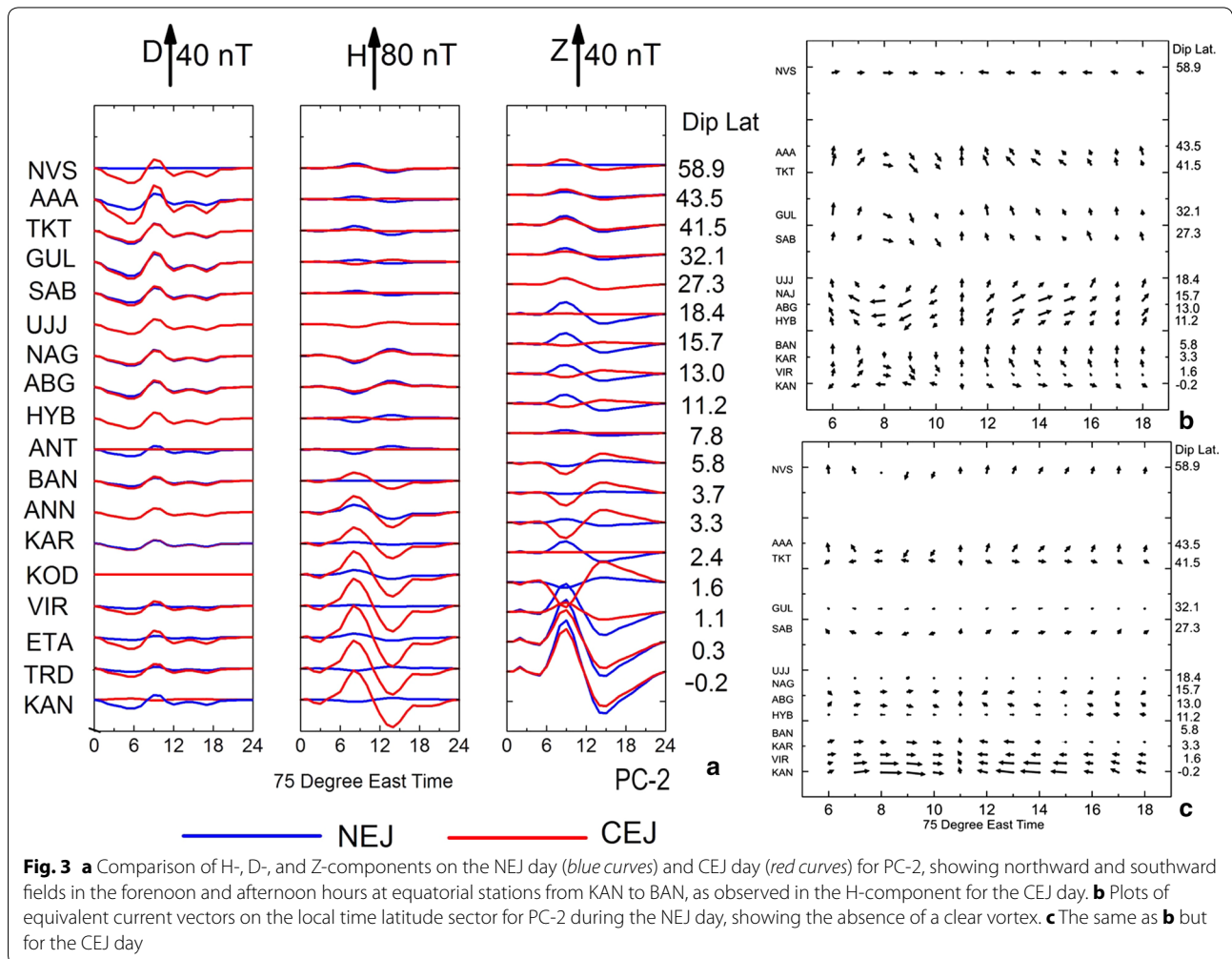titude of NVS, and the expected reversals of the H waveform from "inverted V" type to "V-shaped" are conspicuously absent. The latitudinal differences are more striking in the D-variations at the northern chain of stations. Not only the D-variations are highly subdued during CEJ days, but they are also reversed in comparison with NEJ days, and the diurnal variations are dominated by the early morning minima and afternoon maxima, which indicate westward and eastward magnetic fields that arise due to currents flowing northward in the morning and southward in the afternoon. As shown in Fig. 2a, the amplitudes of the H- and Z-variations for CEJ days are less than those for NEJ days. The overall decrease in the H-component from the dip equator to the focus during a CEJ event may represent magnetic disturbance associated with a ring current or sub-storm activity (Arora et al. 1993). Recently, Chandrasekhar et al. (2017), studying the variability of CEJ signatures between two different longitudes (stations located at Campbell Bay and Vencode), attributed the occurrence of the CEJ to longer wavelength processes such as diurnal and semi-diurnal tides.

Determination of Sq and the CEJ current system

The nature of the Sq current system during an NEJ day (February 6, 1992) along the Indo-Russian longitudinal sector is brought out by the current vector plots as shown in Fig. 2b. The hourly values of H and D, corresponding to PC-1, are combined to produce the magnetic vector, which is rotated by 90° to obtain the equivalent current vector. The equivalent Sq current vector plot for PC-1 clearly shows that the flow path is dominated by an anti-clockwise Sq vortex, with a well-marked focus between GUL and TKT (~35° dip latitude) at about 11 h local time, which is driven by the (1,−2) tidal mode (Stening 1977).

Figure 2c shows the current vector plots for PC-1 for a CEJ day (January 23, 1992) along the Indo-Russian longitudinal sector. The nature of the equivalent CEJ current vector plot for PC-1 does not bring out any clear loop, but most of the current vectors are pointing in an eastward direction in the equatorial region. Its amplitude is less than on an NEJ day.

Figure 3a shows the time variation plots of D, H, and Z for the second principal components for NEJ (blue curves) and CEJ (red curves) days. The D-component for both the NEJ and CEJ days does not show much difference, while the H-component for PC-2 on CEJ days shows abnormal variations (i.e., large negative excursions in the afternoon hours at equatorial stations KAN to BAN), beyond which no variation is evident in PC-2(H). Hence, the CEJ effect is observed in the PC-2(H) component at equatorial stations. The Z-component on CEJ days shows same trend as that on NEJ days for stations TRD and KAN and has the opposite trend for other stations. In Fig. 3b for NEJ days, an anticlockwise loop is observed in the morning hours for PC-2, though this is not clear. Due to the CEJ effect, we do not observe any loop in PC-2 (Fig. 3c), but at equatorial stations the current vectors point eastwards in the mornings and westward in the afternoons, producing northward and southward fields, respectively, in the H-component.

Fig. 3 **a** Comparison of H-, D-, and Z-components on the NEJ day (*blue curves*) and CEJ day (*red curves*) for PC-2, showing northward and southward fields in the forenoon and afternoon hours at equatorial stations from KAN to BAN, as observed in the H-component for the CEJ day. **b** Plots of equivalent current vectors on the local time latitude sector for PC-2 during the NEJ day, showing the absence of a clear vortex. **c** The same as **b** but for the CEJ day

Salient features of the CEJ in the Indo-Russian region

To understand the CEJ effect in all three magnetic components (D, H, and Z), the normal Sq variations were subtracted from the CEJ variations after applying PCA for the corresponding hours, to obtain the difference field as suggested by Bhargava and Sastri (1977). This difference field is due to the counter-electrojet and is shown in Fig. 4a for PC-1. The difference field D in Fig. 4a for PC-1 shows a westward field due to a northward current in the early morning hours and an eastward field due to a southward current in the afternoon, which is characteristic of Sq (D) variations during a CEJ day. The H curves for the difference field show "V"-type variation with minima around noon at equatorial stations and represent a southward field due to a westward current (CEJ). At low-latitude stations, almost constant variations can be seen in the H-field, whereas an inverted "V"-type variation with a noon maximum is observed at midlatitude stations, which is in the opposite direction to the Sq (H) curves as shown in Fig. 2a. The amplitude of the difference field Z is small at the equatorial stations KAN and TRD and the reverse for other stations.

Determination of the CEJ-related equivalent current system

The CEJ-related current system in the Indo-Russian region on January 23, 1992, was determined by subtracting the normal Sq variations from the CEJ variations for the corresponding hours, after applying principal component analysis. The current vector plots for PC-1 are shown in Fig. 4b, which helps to trace the nature of the CEJ-related equivalent current system. The current vector plot for PC-1 (CEJ plot) clearly shows that the flow path is dominated by a clockwise vortex with a well-marked focus around 20°N dip latitude and around 11 h local time. The current flow pattern is dominated by a strip of westward-directed current centered on the dip equator.

Summary

Figure 2 shows NEJ and CEJ day variations along with a current vector plot for PC-1. The current loop brings out the Sq focus around 35° dip latitude between GUL and TKT with an anticlockwise vortex (for NEJ days). CEJ variations for January 23, 1992, for PC-1 are shown in Fig. 2a, where the D-component shows that opposite variations and the amplitudes of the H- and Z-components are reduced, in comparison with the NEJ day (also shown in Fig. 2a). The current loop shown in Fig. 2c does not show any vortex, but the amplitude of the current vectors is reduced and the flow pattern is toward the east. This is due to the enhanced part of the NEJ current, which is westward during CEJ events, whereas the background current density is still eastward as suggested by Fambitakoye and Mayaud (1976).
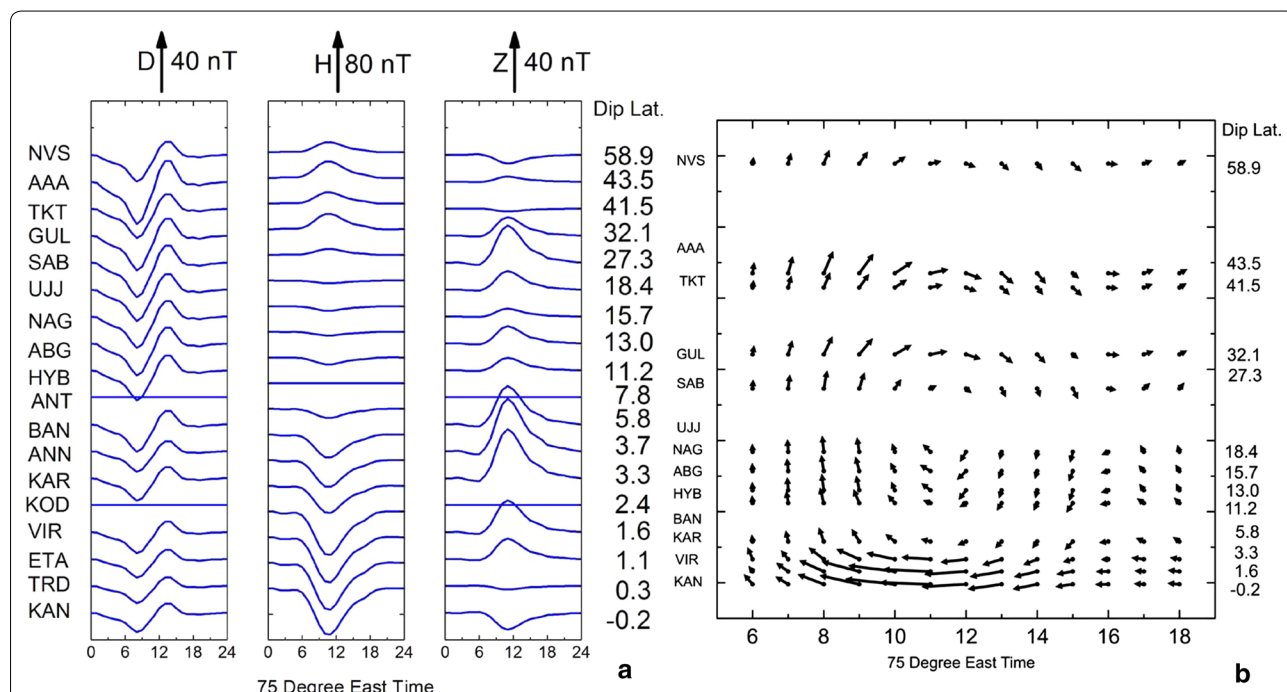

Fig. 4 a Residual fields of CEJ and NEJ days for D-, H-, and Z-components corresponding to PC-1 along the Indo-Russian chain of stations, showing the CEJ effect at equatorial stations extending up to BAN. **b** Plots of equivalent current vectors on the local time latitude sector for PC-1 (for the residual field) during a CEJ day (January 23, 1992) with the focus between UJJ and SAB (~20° dip latitude)

These results indicate that the electric field reversal during CEJ events is confined to electrojet latitudes and can be explained in terms of local winds and the behavior of tidal components at electrojet latitudes (Somayajulu et al. 1993b).

The present observations (Fig. 2a) strengthen the view of earlier researchers (Rastogi 1974; Raghavarao and Anandarao 1987; Rangarajan and Rastogi 1993) that the phenomenon of depression in the H-component of the magnetic field at electrojet stations during afternoon hours is confined up to ANN/BAN (i.e., up to the fringe of the equatorial electrojet) and is a localized event. In the Indian region, the afternoon CEJ has two components: a normal quiet-day electrojet (i.e., NEJ) and an additional field superimposed on it (Bhargava and Sastri 1977).

This additional field is obtained by taking the difference between NEJ and CEJ days for corresponding hours in the D-, H-, and Z-components (for PC-1). This residual field is due to the additional current flowing in a westward direction and is shown in Fig. 4a (for PC-1), and the current loop brings out a focus in between UJJ and SAB (20°N dip latitude) as shown in Fig. 4b on CEJ days.

The change in Sq focus position during CEJ days (as shown in Fig. 4b) is due to intense westward current flow over equatorial latitudes. As observed in Fig. 3a (red curves), an additional field (H-field behavior) is observed northward in the morning and southward in the afternoon, which is superimposed on the normal quiet-day electrojet field. Thus, the observed CEJ effects may have been caused by the additional current system generated by a semidiurnal tidal mode, as reported by Stening (1989) and Stening et al. (1996).

The NEJ current is associated with the (2, 3) tidal mode. Alternation between positive and negative magnetic fields at different times of day explains the afternoon depressions preceded by morning maxima on CEJ days. Enhanced E-W current flow produced by the (2, 3) tidal mode at the equator falls off sharply and reverses direction within ±10° dip latitude. This is consistent with the observation that CEJ-related afternoon minima and morning maxima are confined to a narrow range of latitudes (±5° Dip. Lat.).

Conclusions
Our major conclusions are:

i. Both the EEJ and CEJ current systems have the same latitudinal extent. The anticlockwise and clockwise loops of the ionospheric Sq current system for NEJ and CEJ days are observed, focused around the 35°N and 20°N dip latitudes, respectively, along the Indo-Russian chain of observatories.

ii. The shift in focus on CEJ days is due to additional current systems generated by a semidiurnal tidal mode. The deduced equivalent current pattern brings out the importance of the antisymmetric semidiurnal tidal wind mode in the generation of CEJ events (Stening 1989).

References
Abbas M, Joshua BDB, Adimula IA, Raibu AB, Bello OR (2012) Variability of electrojet strength along the magnetic equator using MAGDAS/CPMN data. J Inf Data Manag 1:10–13

Alex S, Mukherjee S (2001) Local time dependence of the equatorial counter electrojet effect via narrow longitudinal belt. Earth Planets Space 53:1151–1161. doi:10.1186/BF03352410

Alex S, Kadam BD, Rao DRK (1998) Ionospheric current systems on days of low equatorial ΔH. J Atmos Solar Terr Phys 60:371–379

Alken P, Maus S (2007) Spatio-temporal characterization of the equatorial electrojet from CHAMP, Ørsted, and SAC-C satellite magnetic measurements. J Geophys Res 112:A09305. doi:10.1029/2007JA012524

Amory-Mazaudier C, Vila P, Achache J, Achy S, Veka A, AlbouyY Blanc E, Boka K, Bouvet J, Cohen Y, Dukhan M, Doumouya V, Fambitakoye O, Gendrin R, Goutelard C, Hamoudi M, Hanbaba R, Hougninou E, Huc C, Kakou K, Kobea-Toka A, Lassudrie-Duchesne P, Mbipom E, Menvielle M, Ogunade SO, Onwumechili CA, Oyinloye JA, Rees D, Richmond A, Sambou E, Schmuker E, Tirefort JL, Vassal J (1993) International equatorial Electrojet year: the African sector. Rev Bras Geophys 11:303–317

Anandarao BG (1976) Effects of gravity wave winds and wind shears on equatorial Electrojet. Geophys Res Lett 3:545–547

Anandarao BG, Raghavarao R (1987) Structural changes in the currents and fields of the equatorial electrojet due to zonal and meridional winds. J Geophys Res 92:2514–2526

Arora BR, Subba Rao PBV (2002) Integrated modeling of EM response functions from Peninsular India and Bay of Bengal. Earth Planets Space 54:637–654. doi:10.1186/BF03353052

Arora BR, Mahashabde MV, Kalra R (1993) Indian IEEY geomagnetic observational program and some preliminary results. Braz J Geophys 11:365–384

Baker WG, Martyn DF (1953) Electric current in the ionosphere.1. The conductivity. Philos Trans R Soc Lond 246:281–294. doi:10.1098/rsta.1953.0016

Bartels J, Johnston HF (1940) Geomagnetic tides in horizontal intensity at Huancayo. Terr Mag Atmos Elec 45:269–308

Bhardwaj SK, Subba Rao PBV, Veenadhari B (2015) Abnormal quiet day variations in Indian region along 75° E meridian. Earth Planets Space 67:115. doi:10.1186/s40623-015-0292-1)

Bhargava BN, Sastri NS (1977) A comparison of days with and without occurrence of counter electrojet afternoon events in the Indian region. Ann Geophys 33:329–333

Bhargava BN, Sastri NS, Arora BR, Rajaram R (1980) The afternoon counter-electrojet phenomenon. Ann Geophys 36:231–240

Cain JC, Sweeney RE (1973) The POGO data. J Atmos Solar Terr Phys 35:1231–1247

Chandrasekhar NP, Archana RK, Nagarajan N, Arora K (2017) Variability of Equatorial counter electrojet signatures in the Indian region. J Geophys Res. doi:10.1002/2016JA022904

Chapman S (1951) The equatorial electrojet as detected from the abnormal electric current distribution above Huancayo, Peru and elsewhere. Arch Meteorol Geophys Bioclimatol A4:368–390

Chapman S, Bartels J (1940) Geomagnetism, vol 1,2. Clarendon Press, Oxford

Cohen Y, Achache J (1990) New global vector anomaly maps derived from MAGSAT data. J Geophys Res 95:10783–10800

Doumouya V, Vassal J, Cohen Y, Fambitakoye O, Menvielle M (1998) The equatorial electrojet: 1st results from magnetic measurement. Annales de Geophysicae 16:658–676

Doumouya V, Cohen Y, Arora BR, Yumoto K (2003) Local time and longitude dependence of the equatorial electrojet magnetic effects. J Atmos Solar Terr Phys 65:1265–1282

Fambitakoye O, Mayaud PN (1976) The equatorial electrojet and regular daily variation SR:—I. A determination of the equatorial electrojet parameters. J Atmos Solar Terr Phys 38:1–17

Faynberg EB (1975) Separation of the geomagnetic field into a normal and an anomalous part. Geomagn Aeron 15:117–121

Fejer BJ, Farley DT, Balsley BB, Woodman RF (1976) Radar studies of anomalous velocity reversals in the equatorial ionosphere. J Geophys Res 81:4621–4626

Forbes JM (1981) Equatorial electrojet. Rev. Geophysics 19:469–504

Forbush SE, Casaverde M (1961) The equatorial electrojet in Peru. Publ, Carnegie Institute Washington, p 620

Friis-Christensen E, Lühr H, Knudsen D, Haagmans R (2008) Swarm—an Earth observation mission investigating geospace. Adv Space Res 41:210–216

Golovkov VP, Papitashvili NY, Tyupkin YS, Kharin YP (1978) Separation of geomagnetic field variations into quiet and disturbed components by the method of natural orthogonal components. Geomagn Aeron 18:342–344

Gouin P (1962) Reversal of the magnetic daily variation of Addis-Ababa. Nature 193:1145–1146

Gouin P, Mayaud PN (1967) A propos de existence possible d'un contre electrojet et latitudes magnetiques equatorials. Ann Geophys 23:41–47

Guizelli LM, Denardini CM, Moro J, Resende LCA (2013) Climatological study of the daytime occurrence of the 3-meter EEJ plasma irregularities over Jicamarca close to the solar minimum (2007 and 2008). Earth Planets Space 65:39–44. doi:10.5047/eps.2012.05.008

Gurubaran S (2002) The equatorial counter electrojet: part of a worldwide current system? Geophys Res Lett 29:1337. doi:10.1029/2001GL014519

Jadhav G, Rajaram M, Rajaram R (2002) A detailed study of equatorial electrojet phenomenon using Oersted satellite observations. J Geophys Res. doi:10.1029/2001JA000183

Kane RP, Trivedi NB (1982) Comparison of equatorial electrojet characteristics at Huancayo and Eusebio (Fortaleza) in the South American region. J Atmos Solar Terr Phys 44:785–792

Langel RA, Schnetzler CC, Philips JD, Horner RJ (1982) Initial vector magnetic anomaly map from Magsat. Geophys Res Lett 9:273–276

Langel RA, Purucker MM, Rajaram M (1993) The equatorial electrojet and associated currents as seen in MAGSAT data. J Atmos Solar Terr Phys 55:1233–1269

Macmillan S, Olsen N (2013) Observatory data and the Swarm mission. Earth Planets Space 65:1355–1362. doi:10.5047/eps.2013.07.011

Manju G, Viswanathan KS (2005) Short period fluctuations in the equatorial Electrojet electric fields. Ind J Rad Space Phys 35:90–97

Manju G, Pant TK, Devasia CV, Ravindran S, Sridharan R (2009) Electrodynamical response of the Indian low & mid latitude ionosphere to the very large solar flare of 28 October 2003 - A case study. Ann Geophys 27:3853–3860. doi:10.5194/angeo-27-3853

Marriot RT, Richmond AD, Venkateswaram SV (1979) The quiet time equatorial electrojet and counter electrojet. J Geomag Geoelectr 31:311–340

Maynard NC (1967) Measurement of ionospheric currents off the coast of Peru. J Geophys Res 72:1863–1875

Olsen N, Alken P, Beggan CD, Chulliat A, Doornbos E, Encarnação J, Floberghagen R, Friis-Christensen EA, Hamilton B, Hulot G, van den IJssel J, Kuvshinov AVA, Lesur V, Luhr H, Macmillan S, Maus S, Olsen PEH, Park J, Plank G, Püthe C, Ritter P, Rother M, Sabaka TJ, Stolle C, Thebault E, Thomson AWP, Tøffner-Clausen L, Velimsky J, Visser PNAM, Luehr H, Noja M, Puethe C, Rauberg J, Schachtschneider R, Sirol O, Toeffner-Clausen L, Vigneron P, Puthe C, Velímský J (2013) The Swarm satellite constellation application and research facility (SCARF) and Swarm data products. Earth Planets Space 65(11):100. doi:10.5047/eps.2013.07.001

Onwumechili CA (1967) Geomagnetic variations in the equatorial zone. Physics of Geomagnetic Phenomena—I. Academic Press, New York, pp 425–507

Onwumechili CA (1997) The equatorial electrojet. Gordon and Breach. CRC Press, Newark

Raghavarao R, Anandarao BG (1980) Vertical winds as a plausible cause for equatorial counter electrojet. Geophys Res Lett 7:357–360

Raghavarao R, Anandarao BG (1987) Equatorial electrojet and the counter electrojet. Ind J Rad Space Phys 16:54–75

Rajaram M (1980) Method of natural orthogonal components applied to equatorial geomagnetic variations. Ann Geophys 36:599–603

Rangarajan GK, Rastogi RG (1981) Solar flare effect in equatorial magnetic field during morning counter electrojet. Ind J Radio Space Phys 10:190–192

Rangarajan GK, Rastogi RG (1993) Longitudinal difference in magnetic field variations associated with quiet day counter Electrojet. J Geomag Geoelectr 45:649–656

Rastogi RG (1974) Westward Equatorial Electrojet during daytime hours. J Geophys Res 79:1503–1512

Rastogi RG, Deshpande MR, Sastri NS (1975) Solar flare effect in equatorial counter Electrojet current. Nature 258:218–219. doi:10.1038/258218a0

Rastogi RG, Rangarajan GK, Somayajulu VV (1992) Complexities of the counter equatorial electrojet currents. Ind J Radio Space Phys 21:89–96

Rastogi RG, Chandra H, Chakrabarty D, Kitamura K, Yumoto K (2007) Day-to-day variability of the equatorial electrojet current in the South American sector. Earth Planets Space 59:459–461. doi:10.1186/BF03352707

Rastogi RG, Chandra D, Rahul S, Trivedi NB, Fontes SB (2013) A comparison of equatorial electrojet in Peru and east Brazil. Open Atmos Sci J 7:29–36. doi:10.2174/1874282320130417003

Ravat D, Hinze WJ (1993) Consideration of variations in ionospheric field effects in mapping equatorial lithospheric Magsat magnetic anomalies. Geophys J Int 113:387–398

Reddy CA (1981) The equatorial electrojet: a review of the ionospheric and geomagnetic aspects. J Atmos Solar Terr Phys 43:557–571

Reddy CA (1989) The equatorial electrojet. Pure App Geophys 131:485–508

Reddy CA, Devasia CV (1981) Height and latitude structure of electric fields and current due to Local east–west winds in the equatorial electrojet. J Geophys Res 86:5751–5767

Reyment RA, Joreskog KG (1993) Applied factor analysis in the natural sciences. Cambridge University Press, Cambridge

Richmond AD (1973) Equatorial electrojet. I. Development of model including winds and instabilities. J Atmos Solar Terr Phys 35:1083–1103

Rigoti A, Chamalaun FH, Trivedi NB, Padilha AL (1999) Characteristics of the equatorial electrojet determined from an array of magnetometers in N-NE Brazil. Earth Planet Space 51:115–128

Sastry NS, Jayakar RW (1972) Afternoon depression in horizontal component of the geomagnetic field at Trivandrum. Ann Geophys 28:589–591

Singh A, Cole KD (1987) A numerical model of the ionospheric dynamo – III, Electric current at equatorial and low latitudes. J Atmos Solar Terr Phys 49:539–547

Somayajulu VV, Cherian L, Rajeev K, Ramkumar G, Raghava Reddy C (1993a) Mean winds and tidal components during counter electrojet events. Geophys Res Lett 20:1443–1446

Somayajulu VV, Cherian L, Ramkumar G, Reddi CR (1993b) Mean winds and tidal components at Equator during counter electrojet events. Braz J Geophys 11:319–333

Sridharan R, Devasia CV, Jyoti N, Diwakar T, Viswanathan KS, Subbarao KSV (2002) Effects of solar eclipse on the electrodynamical processes of the equatorial ionosphere: a case study during 11 August 1999 dusk time total solar eclipse over India. Ann Geophys 20:1977–1985

Stening RJ (1977) Analysis of contributions to lonospheric dynamo currents from emf's at different latitudes. Planet Space Sci 25:587–594

Stening RJ (1985) Modeling the equatorial electrojet. J Geophys Res 90:1705–1719

Stening RJ (1989) A calculation of ionospheric currents due to semidiurnal antisymmetric tides. J Geophys Res 94:1525–1531

Stening RJ, Reztsova T (2007) The daily variations of the vertical (Z) element of the geomagnetic field around the coast of mainland Australia. Earth Planets Space 59:579–584. doi:10.1186/BF03352720

Stening RJ, Meek CE, Manson AH (1996) Upper atmosphere wind systems during reverse equatorial electrojet events. Geophys Res Lett 23:3243–3246

Sugiura M, Poros DJ (1969) An improved model equatorial electrojet with meridional current system. J Geophys Res 74:4025–4034

Takeda M, Maeda H (1981) Three-dimensional structure of ionospheric currents 2. Currents caused by semidiurnal tidal winds. J Geophys Res 86(A7):5861–5867

Thakkur NK, Alex S (1977) On the movement of northern Sq focus and the semiannualvariations at the equatorial stations. Rivista Italiana di Geofisica, E Scienze Affini 4:128–130

Thakur NK, Mahashabde MV, Arora BR, Singh BP, Srivastava BJ, Prasad SN (1986) Geomagnetic variation anomalies in peninsular India. Geophys J R Astron Soc 86:839–854

Untiedt J (1967) A model of the equatorial electrojet involving meridional current. J Geophys Res 72:5799–5810

Vassal J, Menvielle M, Cohen Y, Dukhan M, DoumouyaV Boka K, Fambitakoye O (1998) A study of transient variations in the Earth's electromagnetic field at equatorial electrojet latitudes in western Africa (Mali and the Ivory Coast). Ann Geophys 16:677–697

Vertlib AB, Wagner CU (1970) Analysis of geomagnetic Sq variations by the expansion of fields in natural orthogonal components I, Method and problems. Geomagn Aeron 10:509–513

Vichare G, Rajaram R (2011) Global features of quiet time counter electrojet observed by Ørsted. J Geophys Res 116:A04306. doi:10.1029/2009JA015244

Vineeth C, Pant TK, Devasia CV, Sridharan R (2007) Highly localized cooling in daytime mesopause temperature over the dip equator during counter electrojet events: first results. Geophys Res Lett 34:L14101. doi:10.1029/2007GL030298

Vineeth C, Pant TK, Sridharan R (2009) Equatorial counter electrojets and polar stratospheric sudden warmings – a classical example of high latitude–low latitude coupling? Ann Geophys 27:3147–3153

Xu WY, Kamide Y (2004) Decomposition of daily geomagnetic variations by using method of natural orthogonal component. J Geophys Res 109:A05218. doi:10.1029/2003JA010216

Yamada Y (2002) 2-day, 3-day, and 5–6-day oscillations of the geomagnetic field detected by principal component analysis. Earth Planets Space 54:379–392. doi:10.1186/BF03352427

Yanagisawa M, Kono M (1985) Mean ionospheric field correction for Magsat data. J Geophys Res 90:2527–2536